Cerebral Cortex, August 2017;27: 4124–4138

doi: 10.1093/cercor/bhw224
Advance Access Publication Date: 13 August 2016
Original Article

ORIGINAL ARTICLE

Spatial Mechanisms within the Dorsal Visual Pathway Contribute to the Configural Processing of Faces

Valentinos Zachariou, Christine V. Nikas, Zaid N. Safiullah, Stephen J. Gotts, and Leslie G. Ungerleider

Laboratory of Brain and Cognition, NIMH/NIH, Bethesda, MD 20892-1366, USA

Address for correspondence to Valentinos Zachariou, Laboratory of Brain and Cognition, National Institutes of Health, Building 10, RM 4C209, 10 Center Drive, Bethesda, MD 20814, USA. Email: zachariouv@mail.nih.gov

Abstract

Human face recognition is often attributed to configural processing; namely, processing the spatial relationships among the features of a face. If configural processing depends on fine-grained spatial information, do visuospatial mechanisms within the dorsal visual pathway contribute to this process? We explored this question in human adults using functional magnetic resonance imaging and transcranial magnetic stimulation (TMS) in a same-different face detection task. Within localized, spatial-processing regions of the posterior parietal cortex, configural face differences led to significantly stronger activation compared to featural face differences, and the magnitude of this activation correlated with behavioral performance. In addition, detection of configural relative to featural face differences led to significantly stronger functional connectivity between the right FFA and the spatial processing regions of the dorsal stream, whereas detection of featural relative to configural face differences led to stronger functional connectivity between the right FFA and left FFA. Critically, TMS centered on these parietal regions impaired performance on configural but not featural face difference detections. We conclude that spatial mechanisms within the dorsal visual pathway contribute to the configural processing of facial features and, more broadly, that the dorsal stream may contribute to the veridical perception of faces.

Key words: face perception, fMRI, spatial perception, TMS

Introduction

Face perception and identification are fundamental functions of the human visual system. These functions appear to be so important that primates have evolved specialized neural machinery within the ventral visual pathway to process faces (Haxby et al. 2000). These face-selective regions in humans span the ventral occipitotemporal cortex and include the occipital face area (OFA; Sergent et al. 1992) within the inferior occipital gyrus, the fusiform face area (FFA; Kanwisher et al. 1997) within the lateral fusiform gyrus, and the anterior inferior temporal face region (Sergent et al. 1992; Haxby et al. 2000), located rostrally within the ventral temporal cortex. All of these regions exhibit disproportionately stronger neural responses to faces compared to non-face categories of objects (Kanwisher et al. 1997; Rossion et al. 2003). Further evidence for dedicated face-selective neural machinery comes from lesion studies, which have shown that damage within ventral occipitotemporal cortex can lead to prosopagnosia, a face-specific perceptual impairment (Della Sala and Young 2003; Duchaine et al. 2006). Prosopagnosic patients are aware that a face is present, but are unable to assign identity to the face. In contrast, they appear to have no impairment in identifying non-face categories of objects (Busigny et al. 2010).

In addition to faces being processed by a distinct neural network of brain regions, the cognitive processes related to face perception appear to differ from those related to other categories of objects. Specifically, faces appear to be processed holistically. That is, during face processing, the features of a face, such as the eyes, nose and mouth, are integrated into a unified whole and the accessibility of information related to individual

facial features is reduced (Maurer et al. 2002). In contrast, in the perception of non-face categories of objects, information related to individual shape features is preserved (Taubert et al. 2011; Kimchi et al. 2012; Zhang et al. 2012).

How this holistic face percept is formed and what specific cognitive processes the face-processing regions mediate remain unclear. One theory suggests that holistic face processing involves at least two cognitive processes: featural processing, which entails perceiving the features of the face, such as the shape of the eyes, nose and mouth, and configural processing, which entails perceiving the spatial arrangement among the facial features, such as the distance between the eyes, nose and mouth (Maurer et al. 2002; Yovel and Kanwisher 2004; Maurer et al. 2007; Zhang et al. 2015).

The processing of face features is associated with the right OFA. For example, transcranial magnetic stimulation (TMS) of the right OFA selectively affects featural but not configural face processing (Pitcher et al. 2007). Similarly, although brain activity within OFA is sensitive to the presence of face parts, it does not appear to be sensitive to their correct within-face configuration (Liu et al. 2010).

The neural substrates responsible for the configural face processing are less clear, but there is some indication that the right FFA may be involved. Multivariate pattern analyses of the brain activity in the right FFA of patients with developmental prosopagnosia implicate impaired configural face processing (Zhang et al. 2015). Neuroimaging studies, however, suggest that the FFA might mediate both featural and configural face processing (Yovel and Kanwisher 2004; Maurer et al. 2007). Lastly, other studies have suggested that configural face processing might be mediated instead by a distributed group of regions that includes the right fusiform gyrus, adjacent to but not overlapping the FFA, and regions in the right frontal cortex (Maurer et al. 2007; Renzi et al. 2013).

The processing of face features is compatible with a primary function of the ventral visual pathway, namely, the processing and perception of shape (Ungerleider and Mishkin 1982). The configural processing of faces is more of a puzzle, in that it likely depends on visuospatial processing, which is not considered to be a primary function of the ventral visual pathway (or of the right frontal cortex). For instance, there is evidence that ventral stream representations of space are mainly topological (e.g., to the left of an item, or on top of an item) and imprecise (Sereno and Lehky 2010). Instead, visuospatial processing is considered to be a primary function of the dorsal visual pathway (Mishkin et al. 1983), in posterior parietal cortex (PPC), such that neurons within this pathway appear to encode and reconstruct stimulus locations with a high degree of spatial precision (Ungerleider and Mishkin 1982; Mishkin et al. 1983; Sereno and Lehky 2010).

The question then arises whether these high-precision spatial mechanisms within the dorsal visual pathway contribute to configural face processing? We explored this question in healthy human adults performing a same-different face detection task while undergoing fMRI and, in a separate experiment, while undergoing TMS.

Materials and Methods

fMRI Experiment

The first step in investigating the contribution of the dorsal stream to configural face processing was to identify and localize brain regions that mediate spatial perception within the dorsal visual pathway and brain regions that mediate face perception within the ventral visual pathway. We could then explore the pattern of activity in response to configural and featural face processing within these localized regions, as well as at the level of the whole brain. Following localization, we presented participants with a same-different face detection task (labeled as the main task), similar to that used in previous studies (Yovel and Kanwisher 2004; Duchaine et al. 2006; Yovel and Duchaine 2006; Maurer et al. 2007; Pitcher et al. 2007; Barton 2008; Liu et al. 2010; Renzi et al. 2013). During the task, in separate, randomized blocks, faces could differ in either their configuration (Fig 1A) or the shape of their features (Fig. 1B). Participants were not instructed to detect configural or featural differences; rather, they were instructed to make same-different judgments on the faces by pressing a button if the faces differed.

Participants

Twenty-one healthy adults (10 female, age range 20–36) participated in the experiment. All were right-handed and had normal vision (corrected, if necessary). Informed consent was obtained from all participants under a protocol approved by the Institutional Review Board of the National Institute of Mental Health.

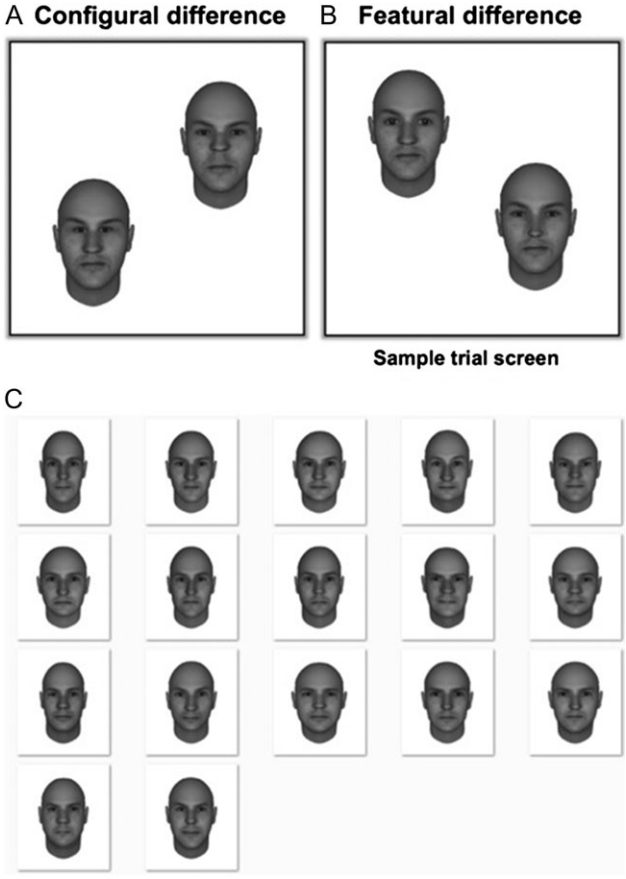

Figure 1. Sample trial screens and face stimuli used in the fMRI and TMS experiments. (*A*) Sample stimulus display used in the main tasks of the fMRI study and TMS experiment, consisting of two face images that differ in the configuration of their internal features (distance between the eyes and between the nose and mouth). (*B*) Sample stimulus display in which the face images differ in the shape of their internal features (eyes and nose). (*C*) All the 20 faces used in the fMRI and TMS experiments.

Procedure

The experiment, implemented using E-prime 2.0, was run on a Windows-7 based PC. Stimuli were presented via an analog projector on a 240 × 180 mm^2 screen (15° visual angle horizontally by 11° vertically at a distance of 92 cm away from the participants' eyes), situated at the bore opening of the MRI scanner at a resolution of 1024 × 768 (0.015° per pixel), 1-ms response time. Participants viewed the projection screen through a mirror attached to the head coil of the MRI scanner. Eye-movement data were collected using an infrared technique (Avotec model RE-5701, Avotec Inc., Stuart, FL).

The localizer and main tasks were split into two, 60-min scan sessions (on different days), with the localizer tasks always preceding the main task. During the localizer session, participants completed four functional runs; two runs per localizer task (described below) and during the main task session participants completed four runs.

Localizer Tasks

Each run of the ventral and dorsal stream localizer tasks consisted of 14 blocks of trials (10 trials per block) in counterbalanced order. Participants were not required to maintain fixation during these trials in order to follow the same experimental procedure as the main task, described below. In both localizer tasks, participants viewed two images presented simultaneously on either side of the screen center for 1.7 s. In half the trials of a block, the images appeared in a top-left, bottom-right configuration and in the remaining half, in a top-right, bottom-left configuration. Each block of trials lasted 22 s and was preceded and directly followed by 8 s of fixation. Trials were separated by 300 msec of fixation.

Dorsal Stream Localizer

For the dorsal stream localizer, we compared activations evoked by a same-different distance detection task with activations evoked by a same-different brightness detection task (adapted from Haxby et al. 1991 and previously used in Zachariou et al. 2015). The two tasks were presented in separate, counterbalanced blocks and were visually very similar: the display consisted of two panels, each containing a dot and a vertical black line. The panels always depicted the dot at opposite horizontal and vertical positions. On each trial, the distance between the dots and lines was randomly drawn from a uniform distribution between 18 and 80 pixels. In addition, the brightness of the dots, on each trial, was randomly chosen to be one of eight brightness levels. Thus, the dot-line distance and dot brightness differed across trials for both tasks. Panels in identical trials in both distance and brightness tasks had the same dot-line distance and the same dot brightness. On each trial, participants compared the two panels and indicated with a button press if the panels differed in distance or brightness.

In same-different distance detection blocks, the brightness of the dot was always identical across the two panels within a trial (but varied across trials), and participants compared the horizontal distance between the dot and the vertical line across the two panels. This horizontal distance differed in half of the trials of each block, and participants indicated detection of this difference by a button press (responses withheld on identical distance trials). A distance difference across panels was created by adding 18–30 pixels (drawn from a uniform distribution) to the original distance between the dot and line in one of the panels.

In same-different brightness detection blocks, the horizontal distance between the dot and the vertical line was always identical across the two panels within a trial (but varied across trials), and participants determined whether the brightness of the dot across the two panels was the same or different. In half of the trials in each block, the dots differed in brightness and participants indicated this by a button press. At the beginning of each block, a dummy trial with either a distance or brightness difference between the panels informed participants of the task in the upcoming block.

The same-different distance detection task was intended to identify cortical regions that process spatial relations between objects compared to regions that are sensitive to changes in brightness, which are anatomically distinct. The same-different brightness detection task, being visually similar to the distance task, (visually identical, apart from the within-trial differences in brightness) was intended as a control and, more specifically, to account for any activity that may not be related to spatial processing per se, such as brain activity related to the shape and overall spatial position of the stimuli in the display.

Ventral Stream Localizer

In the ventral stream localizer tasks we compared activations evoked by a same-different face detection task to activations evoked by a same-different house detection task, thereby identifying regions more active in response to faces compared to a non-face category of objects (the task was adapted from Kanwisher et al. 1997). In separate blocks with counterbalanced order, the presented images depicted either gray-scale images of faces or houses (22 images per category). In half of the trials of each block, the two items differed and participants indicated detection of this difference by button press. Responses were withheld on matching trials. At the beginning of each block, a dummy trial consisting of two different faces or houses (presented for 1.7 s) informed participants of the task in the upcoming block.

Main Task

This task was used to measure activations evoked by configural and featural face difference detections. In each trial, participants compared two faces, presented simultaneously on either side of the screen center, and indicated with a button press if they differed. If they did not differ, participants did not respond. Across trials, the two face images appeared in one of two possible spatial configurations: in half the trials, faces appeared in a top-left, bottom-right configuration, and in the remaining half, in a top-right, bottom-left configuration. The face stimuli were 4.5° wide by 5° long and were separated by 4° of visual angle, 2° on either side of the screen center.

For the main task, we used 20 different face exemplars, which were generated using the FaceGen software package. Following the creation of the face exemplars, we assigned two differently shaped sets of eyes and noses to each one of the 20 faces. Therefore, each face exemplar could appear in two variants, which differed only in the shape of the eyes and the nose. We will refer to the two variants of a face exemplar that differed in shape as S_1 and S_2.

Great care was taken in designing the stimuli of the featural task to ensure that the horizontal distance between the eyes (measured from the inside edge of both eyes) as well as the vertical distance between the top-most part of the mouth and the bottom-most part of the nose were identical between S_1 and S_2.

We achieved this by manipulating the shape of the nose along the horizontal dimension and the shape of the eyes along the vertical dimension (maximum horizontal/vertical distance difference of 0.14° of visual angle between S_1 and S_2). This was done to minimize configural differences when shape was changed in the featural task.

In addition to the two sets of shape features, we also assigned two different spatial configurations to each face exemplar (the difference occurred in the distance between the eyes and between the nose and mouth; typical distance differences were between 0.5° and 0.9° of visual angle). Hence, the shape features (eyes and nose) of each face exemplar could appear with two different spatial configurations. We will refer to these two different spatial configurations as C_1 and C_2.

A featural difference occurred by presenting both the S_1 and the S_2 variants of a face exemplar on the stimulus display of a trial while holding spatial configuration (i.e. C_1 or C_2 randomly selected) constant between the face images. Similar to the featural-difference trials, configural-difference trials occurred when both the C_1 and C_2 spatial configurations of a face exemplar were presented within a stimulus display while S_1 or S_2 (randomly selected) was held constant between the face images.

In no-difference (identical face) trials, both faces on the stimulus display were assigned the same combination of features ($S_{1\ or\ 2}$) and configuration ($C_{1\ or\ 2}$), which were randomly selected. In each block, no difference was present in half the trials.

All face images used in the experiment were in gray-scale (each pixel only carried intensity information, a value from 0% to 100%). Using photoshop, we extracted the per-pixel intensity values of one face image (we used the "save image statistics" function in photoshop), which acted as the template image. The same procedure was used to extract the per-pixel intensity information from the areas of the template face image corresponding to the eyes and nose (separately for each face feature). We then applied these pixel intensity templates (using the same plugin) to every other face image and face feature used in the creation of the S_1 and S_2 variants. Consequently, every face image and face feature was very similar in luminance and contrast to the template face image. The average luminance value of the face images was 40.9%, the variance in luminance was 0.6% and the standard deviation was 0.75%.

Prior to scanning, participants completed a training session that lasted 20–25 min. During training, the running average RT for the two types of face differences was compared. Then, the ratio of configural/featural difference blocks was adjusted to allow more practice for the type of face difference with the slower RT, until the absolute difference in RT was within 100 ms. The RT of a training block was only included in the running average if accuracy was above 90%; if accuracy was below 90%, the training block repeated. If the matching on RT, within the 100 ms criterion, could not be achieved within 15 min of training, participants were presented with configural difference blocks only and the difficulty level of the configural difference trials was adjusted in order to match the RT of featural difference trials. Adjustments in difficulty were made after each block presentation, but if RT could not be matched within a total of 25 min, training was aborted and the participant was excluded from the study. Three participants were excluded for this reason and were not scanned. The difficulty level was controlled automatically and in real-time by the training program and was adjusted by making the two spatial configuration sets, which were assigned to each face exemplar (C_1, C_2), either more similar (increase in difficulty) or more dissimilar (decrease in difficulty). Altering the distance between the eyes and between the nose and mouth controlled the similarity/dissimilarity between spatial configurations. If difficulty changes occurred, they did so for all configuration sets, across all face exemplars and feature sets.

A functional run of the main task consisted of twelve, 32-s blocks, each preceded and followed by 8 s of fixation. Each trial lasted 2700 ms and trials within a block were separated by a 300 ms intertrial interval. Participants were never told about the two types of face differences and were only asked to make same-different judgments between faces (We had piloted a version of the main task performed at fixation with a time delay between stimuli, but it did not go well: at short delays between sample and target, apparent motion was visible for the configural task (the eyes and nose appeared to move). We eliminated this apparent motion effect with a mask presented between the sample and target and a delay of about one second. At this long delay, however, memory mechanisms came into play, such as encoding of the sample stimulus into short-term memory, maintenance of the sample stimulus trace, and the comparison of the sample stimulus to the target stimulus currently on the screen. All of these memory mechanisms could interact with the type of task (configural/featural) in an fMRI experiment. We therefore opted for the simpler experimental design. We outline above, in which memory would contribute minimally to brain activations. Consequently central fixation was not required in any of the tasks. With stimuli presented at either side of the screen center, it is very difficult to perform the tasks while maintaining fixation.).

Same-Different Face Detection Control Tasks

Two additional same-different face detection control tasks were run in order to obtain face-related BOLD activations in individually defined FFA in response to different face identities. These control tasks were used to compare face-related activity in FFA resulting from the presentation of different faces to the activity evoked when faces differed in features or configurations only. This comparison acted as a measure of the similarity of the featural/configural face task to more conventional face discrimination tasks. Both of these control face tasks had a similar procedure to that of the ventral localizer tasks: in one of the tasks, in separate blocks with counterbalanced order, the presented images depicted either gray-scale images of faces (never seen before) or houses (20 images per category). In the other task, the presented images were the face stimuli used in the main fMRI task and gray-scale images of chairs was the non-face category (20 images per category). In half of the trials of each block, the two items differed (two different faces, or houses, or chairs) and participants indicated detection of this difference by button press. Responses were withheld on matching trials. Both of these control face tasks consisted of four functional runs. A functional run of both face tasks consisted of twelve, 32-s blocks, each preceded and followed by 8 s of fixation. Each trial lasted 2700 ms and trials within a block were separated by a 300-ms intertrial interval, following the same procedure as the main task of the fMRI study. The control face tasks were presented in counterbalanced order across participants but both control tasks occurred chronologically after the main fMRI and TMS tasks and the localizers described earlier in the Methods section.

fMRI Acquisition

Participants were scanned in a General Electric MR750 3 T scanner with a 32-channel head coil. Functional images were

acquired with an echo-planar imaging sequence (TR=2 s, TE = 27 ms, flip angle 79°, 3.2 mm isotropic voxels, 72 × 72 matrix, field of view 230 mm, 45 axial slices covering the whole brain). The 45 slices were acquired with in-plane acceleration, using the GE protocol ASSET (http://www.gehealthcare.com/usen/education/tip_app/docs/fieldnotes_volume1–1_asset.pdf) with an acceleration factor of 2. An MPRAGE and a proton density sequence (1-mm^3 voxels; 176 slices, field of view 256 mm) were used for anatomical imaging and were acquired within the same scan session (MPRAGE and proton density scans were collected in both the localizer and main task sessions).

fMRI Pre-processing

Structural scans were first corrected for the 32-channel head coil contrast artifacts using the proton density scan acquired during each session. The functional scans were then slice scan-time corrected, motion corrected, co-registered to their constituent contrast-corrected anatomical image, normalized to Talairach space (Talairach and Tournoux 1988) using a non-linear transformation (3dQwarp; http://afni.nimh.nih.gov/pub/dist/doc/program_help/3dQwarp.html), smoothed with a Gaussian kernel of 6.0 mm FWHM and mean-based intensity normalized (all volumes by the same factor) using AFNI (Cox 1996). In addition, linear and non-linear trends (where necessary) were removed during pre-processing of the data.

Additional pre-processing steps were performed prior to the functional connectivity analysis, according to the basic ANATICOR regression-based approach (e.g. Jo et al. 2010; Gotts et al. 2012; Stoddard et al. 2016). Using each participant's anatomical scan (MPRAGE), ventricles, gray and white matter segmentation masks were created (using SPM8; http://www.fil.ion.ucl.ac.uk/spm/software/spm8/) separately for each participant. All masks were resampled to the EPI voxel resolution, and ventricle and white matter masks were eroded by one voxel to prevent partial volume effects with gray matter. We then extracted separate nuisance time series for ventricles and white matter. In total, the nuisance regression for each participant involved 11 regressors of no interest: six motion parameters, one average ventricle time series, one localized estimate of white matter (averaging within a sphere of radius 20 mm centered on each voxel), and the first three principal components of all voxel time series from a combined ventricle and white matter mask, calculated after first detrending with AFNI's fourth-order polynomial baseline model (as in Stoddard et al. 2016; comparable to aCompCor: Behzadi et al. 2007). After this nuisance model was subtracted from each participant's EPI data to obtain the cleaned residual time series, a task regression was performed to further remove any evoked responses from the blocks during the task (using the BLOCK model in AFNI's 3dDeconvolve). The resulting time series were then extracted separately from blocks of different conditions, with blocks of the same type concatenated together for purposes of condition comparisons after adjusting for the delay in the BOLD signal in each block (six seconds after the start of each block until four seconds after then end). Estimates of the level of residual global artifacts present in the residual time series (including factors such as head motion, cardiac and respiration effects, etc.) were calculated per condition for later use as nuisance covariates in group-level analyses using the global level of correlation or "GCOR" (e.g. Gotts et al. 2013; Saad et al. 2013), which is the grand average correlation of all voxels with each other (gray matter voxels).

fMRI Statistical Analyses

All imaging data were analyzed using AFNI (Cox 1996). Data from the localizer and main task were analyzed using linear mixed-effects models (*3dLME*; Chen et al. 2013). The resulting statistical maps were thresholded at a family-wise error corrected $\alpha < 0.01$ at $p < 0.001$, using the AFNI program *3dClustSim* (http://afni.nimh.nih.gov/pub/dist/doc/program_help/3dClustSim.html). Alpha (α) denotes the false positive rate at the cluster level. That is, α is the probability of false positives associated with all the clusters that are above the minimum cluster size (estimated from 3dClustSim using Monte Carlo simulations) for a specific voxel-wise (uncorrected) p-value threshold.

The motion parameters from the output of the volume registration step were regressed out in all AFNI analyses.

The analyses at the individual subject level were performed as follows: First, we identified the right FFA and spatial processing regions within the right PPC at the individual subject level using the ventral and dorsal stream localizer data (positive values from the fMRI contrasts of same-different faces > same-different houses and same-different distance detections > same-different brightness detections). Following localization, 60-voxel wide spheres were centered at the peak voxel of each individually defined right FFA and right PPC and we averaged the beta-weight coefficients for configural and featural difference detections within each sphere. The sphere approach was used so that all participants would have an average activity measure from an equal number of voxels between the ventral and dorsal ROIs. Lastly, a repeated measures ANOVA was conducted on the average brain activity between type of face difference (configural or featural) and ROI (right FFA or right PPC).

Brain-behavior correlations were analyzed using linear mixed-effects models (*3dLME;* Chen et al. 2013), ANCOVAs using the AFNI program 3dttest++ (http://afni.nimh.nih.gov/pub/dist/doc/program_help/3dttest++.html) and the SPSS software package where necessary. The resulting statistical maps were thresholded at a family-wise error corrected $\alpha < 0.01$ at $p < 0.001$.

Seed-to-whole-brain functional connectivity analyses using the right FFA as a seed were performed as follows. First, brain masks were created for each participant that comprised gray-matter voxels only (using SPM8). Then, using the 60-voxel wide spheres centered at the peak voxel of each individually defined right FFA (described earlier), seed time series were extracted and then correlated (Pearson's r) with the cleaned residual time series in all gray matter voxels (described in the pre-processing section). Correlation maps with the right FFA were calculated separately for featural and configural face difference detections and separately for each participant. The maps were then transformed using Fisher's Z to yield normally distributed values. A group-level analysis was then performed, using linear mixed-effects models (*3dLME;* Chen et al. 2013), contrasting the correlation maps from configural difference detections to those of featural difference detections both in the entire gray-matter mask as well as within a mask constructed by the localizer defined ROIs (bilateral PPC, bilateral FFA and bilateral PPA ROIs). In order to rule out contributions of global BOLD artifacts (e.g. head motion, cardiac/respiration fluctuations) to the condition differences, GCOR (described in the pre-processing section) was added as a nuisance covariate to these condition comparisons (Gotts et al. 2013).

Behavioral data collected during a scan were analyzed using SPSS and a general linear mixed-effects model (with participants added as a random variable). Multiple comparisons used Sidak corrections where necessary.

The eye-tracking data were analyzed using the Open Gaze And Mouse Analyzer package (OGAMA; Voßkühler 2009). The following procedure was used to compare the pattern of eye fixations between the configural and featural difference tasks across trials. For each of the four on-screen locations where face images could appear (two locations per trial), 9 areas-of-interest (AOIs) were constructed in a 3 × 3 matrix, covering the entire region occupied by a face image (36 AOIs in total). The width of all AOIs was 2.0° of visual angle and their height was 2.5°. An additional AOI with similar dimensions was placed at the center of the screen, at the same location where a fixation cross appeared between trials of the main task.

The number of eye fixations, fixation duration and duration to first fixation in each AOI, for each type of face difference, were calculated for each participant. ANOVAs were then conducted separately for each dependent measure with type of face difference and AOI (1–37) as factors. In addition, in a separate ANOVA analysis, we contrasted the average saccade lengths between configural and featural difference detections.

TMS Experiment

To further evaluate whether the spatial processing regions of the dorsal stream contribute to configural face processing, we investigated the effect of TMS of these regions on configural and featural face difference detections using the same experimental procedure as in the fMRI study.

Participants

Twenty healthy adults (11 female, age range 22–41), who did not take part in the fMRI study, participated in the TMS experiment. All were right-handed and had normal vision (corrected, if necessary). Informed consent was obtained from all participants under a protocol approved by the Institutional Review Board of the National Institute of Mental Health.

Procedure

The experiment, implemented using E-prime 2.0, was run on a Windows-7 based PC. Stimuli were presented on a 120 Hz display (25° visual angle horizontally by 19° vertically at a distance of 90 cm away from the participants' eyes), 3-ms response time computer display at a resolution of 1024 × 768. The size of each face image on the screen was 4.5° horizontal by 5° vertical.

Dorsal Stream Localizer

The dorsal stream localizer tasks used in the fMRI study were also used in the TMS experiment to identify the regions within PPC more strongly activated in response to same-different distance detections compared to same-different brightness detections. Target sites for TMS were then selected bilaterally and corresponded to the peak activity voxels within left and right PPC. TMS target sites were selected at the individual subject level. The vertex, the top most center part of a participant's head, defined as the midpoint between the inion and the nasion of the head, was used as the control TMS site.

The right OFA could potentially be a better control brain region for the TMS experiment in comparison to the vertex, since TMS on the OFA could reveal a double dissociation between featural and configural face processing; TMS on the right OFA has been shown to impair performance on featural but not configural face processing (Pitcher et al. 2007) whereas TMS on the PPC sites could show the reverse effect. Unfortunately, however, the OFA is situated anatomically in the vicinity of the neural foramen, right below the skull base where the facial nerve runs. TMS stimulation at this site causes the face to jerk and, according to our participants who have experienced TMS to OFA, it is painful. During pilot runs of the TMS experiment, we stimulated a few volunteers on their localized right OFA, and all reported a discomfort rating of 10/10 (compared to 2–3/10 for the PPC and vertex TMS sites). In addition, some of those individuals reported headaches the next day. Accordingly, we decided to switch control regions from the OFA to the vertex.

Brainsight V2 (Rogue research, Montreal, Canada) was the navigator program used to position the coil for stimulation and this position was monitored in real-time during the experiment. For the PPC TMS sites, the coil was oriented with an angle of approximately 45° from the nasion-inion line with the handle pointing towards the back of the participants. For the vertex TMS site, the coil was oriented tangentially to the scalp and parallel to the nasion-inion line with the handle of the coil pointing towards the right-hand side of the participants.

Main Task

The main task used in the TMS experiment was very similar to the one used in the fMRI study, with a few changes to make the experimental procedures compatible with approved NIMH-IRB TMS protocols and similar to those in previous TMS studies exploring face perception (e.g. Pitcher et al. 2007; Silson et al. 2013). First, stimulus duration was maintained at 2700 msec, similar to the fMRI study, but the face stimuli only appeared for the first 500 ms of that time. Like the fMRI study, participants were allowed to respond at any time during the 2700 ms of a trial and were explicitly instructed that it was not necessary for them to wait until the stimuli disappeared before responding. Second, the intertrial interval was longer and randomly varied between 4600 ms and 5800 ms in order to conform to the TMS safety guidelines (Wassermann 1998; Rossi et al. 2009). Jittering of the intertrial interval was used so that participants could not predict when the next TMS pulse train would be delivered. The same independent variables were, as in the fMRI study, type of face difference, and here additionally TMS (administered or not) and TMS site (left PPC, right PPC and vertex). TMS was administered at the block level (administered in all trials within a block or in none). TMS site varied at the level of a run and each run consisted of eight blocks of trials (two blocks per condition in randomized order: configural difference detections with and without TMS and featural difference detections with and without TMS). Blocks of trials were separated by 8 s of fixation and runs were separated by a two-minute break, which facilitated the placement of the TMS coil to a new site. Two TMS coils were used during the experiment, switched at the end of a run and the TMS coil order was counterbalanced across participants. The TMS site was also counterbalanced across participants but TMS on the vertex was delivered in a different session, on a different day. The reason for the different sessions was that we were unable to keep the TMS coils cool enough for all three TMS sites to be stimulated within a single session. Consequently, we delivered TMS to the vertex site on a different day. An equal number of participants (randomly assigned) started with TMS on the vertex site and on the PPC sites (left/right site was counterbalanced across participants within a session) and participants were unaware of the TMS site order and which TMS site was the control

(participants were not told that a control TMS site was used). During TMS trials, five TMS pulses were delivered at 10 Hz (one pulse every 100 ms) starting with stimulus onset.

Prior to the main TMS task, participants completed a training session that lasted 30–35 min. This training session was identical to the one used in the fMRI study with the exception that the accuracy criterion was set to 75% instead of 90%, and the training program stopped the training after 35 minutes instead of after 25 min.

TMS Protocol

TMS was delivered as a train of five, biphasic (equal amplitude) TMS pulses at 10 Hz (pulses were separated by 100 ms) at 70% of the maximum stimulator output (1.7 Tesla). Pulses were delivered using a figure-eight coil (70 mm external diameter) in conjunction with a Magstim Super Rapid stimulator with four boosters attached.

Statistical Analyses

The behavioral data collected during the TMS experiment were analyzed using SPSS and a general linear mixed-effects model (with participants added as a random variable), similar to the analysis of the behavioral data in the fMRI study. Multiple comparisons used Sidak corrections where necessary.

Results

fMRI Experiment

Localizer Tasks

Dorsal stream localizer task. The dorsal stream localizer task compared activations evoked by a same-different distance detection task (intended to identify brain regions that process spatial relations between objects) with activations evoked by a same-different brightness detection task.

Activation maps were created at the group level using the fMRI contrast of same-different distance detections > same-different brightness detections. A single mask, which served as the dorsal stream ROI, was created from all positively activated regions (Fig. 2A): bilateral precuneus and superior parietal lobule (bilateral BA 7) and right inferior parietal lobule (right BA 40).

Ventral Stream Localizer Task

A face-localizer task compared activations evoked by a same-different face detection task (the face stimuli differed from those used in the main task) with activations evoked by a same-different house detection task.

Activation maps were created at the group level using the fMRI contrast of same-different face detections > same-different house detections. Positively activated regions included bilateral fusiform gyrus (bilateral BA 20 and 37), whereas negatively activated regions included bilateral parahippocampal gyrus (bilateral BAs 36 and 37) and bilateral lingual gyrus (bilateral BA 18). A single ROI was created from the regions more strongly active in response to faces (Fig. 2A).

Main Task

Activation maps were created at the group level first, using the fMRI contrast of configural differences > featural differences (Fig. 2A); positive activations corresponded to regions more active in response to configural difference detections, while negative activations corresponded to regions more active in response to featural difference detections. There was significantly stronger activation in response to configural difference relative to featural difference detections within PPC; specifically, stronger activation for configural than featural difference detections were observed within bilateral precuneus, superior parietal lobules and right inferior parietal lobule (bilateral BA 7 and right BA 40), which almost entirely overlapped the regions identified by the dorsal stream localizer task.

In addition to the above regions, we observed stronger activation for configural than featural difference detections within the right middle frontal gyrus (within 4 mm of BA 6), right middle temporal gyrus (BA 19) and right superior occipital gyrus (BA 19). To evaluate the functional contribution of these regions, we performed a meta-analysis using the linkRbrain database (for the meta-analysis, we uploaded the entire activation pattern from the right middle frontal gyrus, right middle temporal gyrus and right superior occipital gyrus to the linkRbrain database; http://www.linkrbrain.xyz). The results

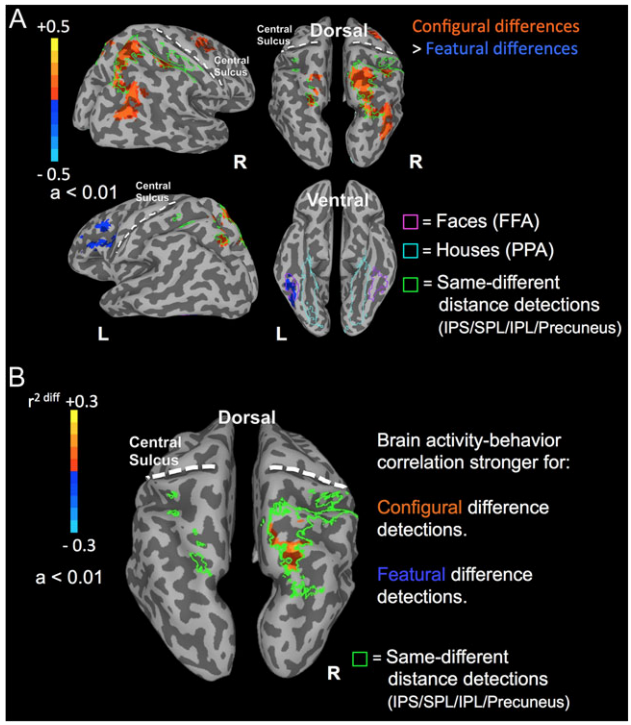

Figure 2. Cortical activation and brain activity–behavior correlation maps from the fMRI study. The 3D cortical meshes shown are partially inflated so activity within the sulci can be visible. (A) Cortical activation maps (magnitude of activity; difference in beta-weight coefficients) revealed by the fMRI contrast of configural difference detections > featural difference detections at the level of the whole brain (B) Correlation maps revealed by the interaction term in the linear mixed effects model contrasting the brain activity-behavior correlations between the two face tasks. Positive activations (yellow-orange) correspond to regions, within the localized dorsal ROI, where the correlation between brain activity (beta-weight coefficients) and RT (msec) was stronger for configural compared to featural face difference detections (the unit is difference in r^2 values). Negative activations (cyan-blue) correspond to regions, within the dorsal ROI, where the correlation between brain activity (beta-weight coefficients) and RT (ms) was stronger for featural compared to configural face difference detections. The green outlines illustrate the brain regions identified by the dorsal stream localizer tasks (IPS, intraparietal sulcus; SPL: superior parietal lobule; IPL: inferior parietal lobule). The pink and cyan outlines illustrate the brain regions identified by the ventral stream localizer tasks (pink: stronger activation in response to faces; FFA: fusiform face area; cyan: stronger activation in response to houses; PPA: parahippocampal place area). For clarity, the anatomical locations of the central sulci are shown with dashed white lines.

from the meta-analysis indicated that the activity observed within the right middle frontal gyrus has been previously associated with visuospatial working memory (for example Olesen et al. 2004). The activity observed within the right middle temporal gyrus and right superior occipital gyrus has been associated with a large number of different cognitive functions; however, the strongest correlation between the activity patterns we observed ($r = 0.21$) and activity reported in previous studies was with mental rotation tasks (e.g. Gauthier et al. 2002).

In contrast to the regions showing greater activations to configural than featural difference detections, activations were greater in response to featural difference detections in the left mid-fusiform gyrus, which overlapped the left FFA identified by the face-localizer task. These greater activations within the left FFA to featural differences replicate the findings of previous studies (Rossion et al. 2000; Harris and Aguirre 2010). Greater activation for featural than configural difference detections was also observed in the left inferior frontal gyrus (BA 9), an area considered to be part of the extended face network (Haxby et al. 2000; Fox et al. 2009).

Unlike the left FFA, at the group level, we did not observe any significant brain activity within the right FFA, indicating one of two possibilities: (1) the right FFA was not activated by either configural or featural face difference detections; or (2) the right FFA was activated to the same extent by configural and featural face difference detections. To differentiate between these two possibilities, we ran an additional, ROI analysis, focused on brain activity within the right FFA and right PPC ROIs (individual subject ROI definitions are described in the methods).

The analysis yielded a significant interaction of ROI (right FFA vs. right PPC) by type of face difference (featural or configural; ($F(1,20) = 39.8$, $p < 0.01$) with ROI as the only significant main effect ($F(1, 20) = 32.5$, $p < 0.01$; average beta-weight coefficient for right FFA: 0.73; average beta-weight coefficient for right PPC: 0.20). Type of face difference was not a significant main effect ($F(1,20) = 1.82$, $p = 0.19$). To further explore the significant interaction, we ran paired t-tests between the activity evoked by configural and featural difference detections in each ROI separately. For the right FFA, the paired t-test yielded no significant results ($t(20) = -1.72$, $p = 0.10$; average beta-weight coefficient for configural difference detections: 0.72; average beta-weight coefficient for featural difference detections: 0.74). In contrast, the analysis for the right PPC was significant ($t(20) = 4.14$, $p < 0.01$; average beta-weight coefficient for configural difference detections: 0.34; average beta-weight coefficient for featural difference detections: 0.06). These results thus indicate that the right FFA was robustly but equally active in response to configural and featural face difference detections, which is in accord with previous findings (Yovel and Kanwisher 2004; Maurer et al. 2007). In contrast, and parallel to the group-level analysis, the right PPC was more strongly active in response to configural relative to featural face difference detections.

Main Task Brain Activity–behavior Correlations

As a next step in exploring the functional contributions of dorsal stream regions to configural face processing, we correlated the fMRI activity in response to configural and featural face difference detections with behavioral performance, using RT (ms) as the behavioral measure. We chose RT because it had greater variability compared to accuracy and was therefore a good candidate for a correlation analysis. Correlations were first performed at the voxel level and at the level of the whole brain: separate correlation analyses were performed between brain activity and RT at each voxel, constrained within gray-matter voxels only (i.e., we ran per-voxel ANCOVAs). The resulting brain activity–RT correlation maps were then clustered and adjusted for multiple comparisons (using family-wise error correction; $\alpha < 0.01$ at $p < 0.001$). The linear mixed model used (see Methods) was constructed using one factor and one covariate: brain activity (beta-weight coefficient) for type of difference (configural/featural) was the factor and RT (msec) for each type of face difference was the covariate. The model tested for both main effects and interactions between the factor and covariate.

At the level of the whole brain, the brain activity–RT correlations did not survive the multiple comparisons correction and we did not observe any significant results. Subsequently, we repeated the correlation analysis within a smaller size mask, comprised of the ROIs identified by the localizer tasks (the ROIs identified by the face-, house-, and distance-difference detection tasks), in order to reduce the number of statistical comparisons to those voxels of most interest. A significant fMRI activity–RT interaction was observed within the localized, right PPC (Fig. 2*B*); specifically, within the right precuneus (right BA 7), the correlation between brain activity (beta-weight coefficients) on configural face difference detections trials and RT (on these same trials) was stronger compared to the correlation between brain activity on featural face difference detection trials and RT (on these same trials). The correlation between brain activity in response to configural difference detections and RT was positive (r^2 of most significant voxel = 0.3, within the right precuneus; the threshold was set to $\alpha < 0.01$ at $p = 0.001$). Those participants with greater activation in response to configural difference detections were slower (longer RTs) at detecting configural face differences. This finding is consistent with previous literature showing that longer RTs correlate with greater magnitude of task-related hemodynamic responses (Yarkoni et al. 2009; Rao et al. 2013; Domagalik et al. 2014). The brain activity–RT correlation between featural difference detections and RT was not significant within the dorsal stream ROIs (r^2 of most significant voxel = 0.14, within the right superior parietal lobule, 1 mm away from the right BA 7; $\alpha > 0.05$ irrespective of uncorrected p value). Consequently, the significant interaction we described earlier was driven primarily by the significant brain activity–RT correlation between activity for configural difference detections and constituent RT within the right precuneus.

In contrast to the dorsal stream ROIs, we did not find any significant brain activity–RT correlations or brain activity–RT interactions between configural/featural face difference detections within the ventral stream ROIs. A similar lack of brain activity–RT correlations in response to configural and featural difference detections within the ventral visual pathway has also been reported by Maurer et al. (2007) and could be indicative of at least two (not mutually exclusive) possibilities: (1) presenting faces that differ only in spatial configuration or facial features poorly activates the face processing regions (such as bilateral FFA), compared to presenting completely different faces; or (2) the variability in the magnitude of brain activity within the ventral stream ROIs maybe smaller compared to that in the dorsal stream ROIs, leading to poor brain activity–RT correlations.

To address these two possibilities, we ran two additional analyses, described below. First, using BOLD activity from the same-different face detection control tasks, described in the Methods, we individually defined the right FFA twice; once,

using activation evoked by faces > houses as the BOLD contrast and then again using activation evoked by faces > chairs (all ROIs were family-wise error corrected at $\alpha < 0.01$, $p < 0.001$). The right FFA ROIs, individually defined from the faces > houses BOLD contrast, were then used to extract beta-weight coefficients from the faces-chairs task and the right FFA ROIs, individually defined from the faces > chairs BOLD contrast, were used to extract beta-weight coefficients from the faces-houses task (for both the face and non-face category in each task). Lastly, using the right FFA ROIs defined from the faces > houses BOLD contrast, we extracted beta-weight coefficients from the configural and featural difference detection blocks of the main task of the fMRI study.

A repeated measures univariate ANOVA analysis was then run using face activity as the sole factor, consisting of the following four levels: face activity from the faces versus houses task, face activity from the faces versus chairs task, and face activity from configural and featural difference detection tasks. The analysis on the face activity factor did not yield a significant main effect [$F(3, 80) = 3.29$, $p = 0.09$; % BOLD signal change of face activity: from the faces vs. houses = 1.17; faces vs. chairs task = 1.00; configural difference detections = 0.89, featural difference detections = 0.89]. Thus, the face-related activity observed during configural and featural difference detections in individually defined FFAs was comparable in magnitude to the activity in FFA when participants performed same-different detections between two different faces. Hence, the lack of significant brain activity–RT correlations in ventral temporal cortex, including FFA, cannot be explained by poor BOLD activation in response to configural and featural difference detections within the ventral stream ROIs.

To evaluate the second possibility for the absence of significant brain activity–RT correlation in ventral stream ROIs, we assessed whether the variability in the magnitude of activation in the ventral stream ROIs was similar to that in the dorsal stream ROIs by using the Levene's test of homogeneity of variance. The test of homogeneity of variance was significant (Levene statistic = 13.93, $p = 0.001$). The variance of the beta-weights in the ventral stream ROIs was 0.14, whereas the variance of the beta-weights in the dorsal stream ROIs was 0.03 (almost five times smaller). Consequently, since activity in the ventral ROIs had greater variability compared to the dorsal ROIs, a lack of sufficient variability in the magnitude of brain activity within the ventral ROIs cannot explain why we did not observe significant brain activity–RT correlations within these regions. We discuss this point further in the Discussion.

Main Task Functional Connectivity Analyses

In order to explore possible interactions between the face processing regions of the ventral stream and the spatial processing regions of the dorsal stream, we performed the following connectivity analysis. Here, using a linear, mixed-effects model, we explored how the functional connectivity patterns between individually defined FFA and the rest of the brain (see Methods) differed between configural and featural face difference detections. All resulting maps from the functional connectivity analyses were adjusted for multiple comparisons using the family-wise error correction ($\alpha < 0.05$ at $p < 0.001$).

At the level of the whole brain, the results from the connectivity analysis did not survive the multiple comparisons correction. We then repeated the analysis within a smaller mask of the previously localized ROIs (the same mask used earlier in the brain activity–RT correlation analyses) in order to reduce the number of statistical comparisons to those voxels of most interest. The correlations observed between the brain activity in the right FFA seed region and the activity of voxels within the localized ROIs for both configural and featural difference detections were positive. Within the posterior parietal ROIs, identified using the same-different distance detection localizer, the functional connectivity between the right FFA and the right superior parietal lobule (BA 7) was significantly stronger during configural face difference detections compared to featural face difference detections (peak difference in Pearson's $r = 0.1$; Fig. 3A). In contrast, the functional connectivity between the right FFA and the left FFA ROIs was significantly stronger during featural face difference detections compared to configural face difference detections (peak difference in Pearson's $r = 0.07$; Fig. 3B). The pattern of connectivity between the right FFA and either the left or right PPA ROI was not significant.

Thus, the functional connectivity analyses revealed the following. As would be expected, during featural face difference detections, the right FFA showed greater functional connectivity with other face processing regions of the ventral stream. In contrast, during configural face difference detections, the right FFA showed greater functional connectivity with the spatial processing regions of the dorsal visual pathway. Second, we explored the relationship between the difference in average FD between the two face conditions (configural and featural face difference detections) to the difference in the functional connectivity (the Pearson r values) between the two condition

Transient Head Motion Comparison Between Configural and Featural Difference Detections

To ensure that transient head motion was not driving the functional connectivity findings described above, we performed two

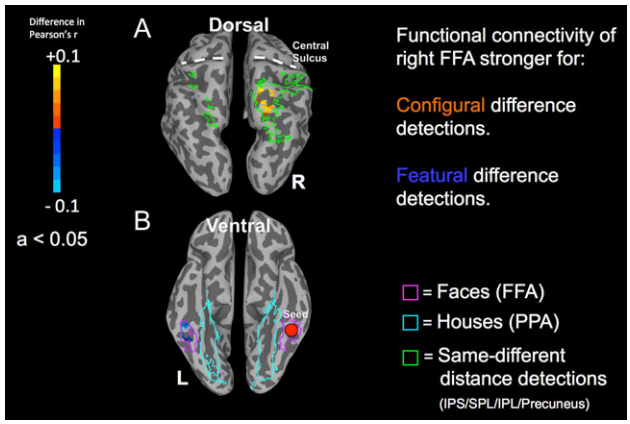

Figure 3. Differences in functional connectivity for configural and featural face difference detections between the right FFA (individually localized) as the seed and BOLD activity in: (A) brain regions identified by the dorsal stream localizer task (IPS, intraparietal sulcus; SPL: superior parietal lobule; IPL: inferior parietal lobule; shown as green outlines); and (B) brain regions identified by the ventral stream localizer task (pink: greater activation in response to faces; FFA: fusiform face area; cyan: stronger activation in response to houses; PPA: parahippocampal place area). Positive activations (yellow-orange) indicate that functional connectivity between the activated voxels and those within the right FFA seed region was stronger during configural face difference detections compared to featural difference detections (a difference in Pearson's r). Negative activations (cyan-blue) indicate that functional connectivity between the activated voxels and those within the right FFA seed region was stronger during featural face difference detections compared to configural difference detections. For clarity, the anatomical locations of the central sulci are shown with dashed white lines.

control analyses with frame-wise displacement (FD; expressed in mm per TR) as a measure of transient head motion. In the first analysis we compared the average FD between configural and featural face difference detection trials, across participants, using a paired-samples t-test. The paired-samples *t*-test indicated that the two conditions were well matched on average FD: Configural face difference detections: 0.104 mm/TR; Featural face difference detections: 0.105 mm/TR; paired $t(20) = 1.41$, $p = 0.17$.

In the second analysis, we explored the relationship of condition differences in FD per subject to condition differences in functional connectivity between the right FFA (the seed region). The initial functional connectivity analysis yielded two significant clusters, within the localized ROI mask. Namely, one cluster was identified within the right precuneus (BA7) and another cluster within the left localized FFA. Using these significantly active clusters, we created two new ROIs. We then explored, in each of these two ROIs separately, if the difference in functional connectivity with the right FFA (differences in Pearson's *r*) between configural and featural difference detections correlated significantly with the difference in FD between the same conditions, across participants. The correlation across subjects between the change in FD between conditions and the change in functional connectivity with the right FFA between conditions was not significant: right PPC ROI: $r(19) = 0.37$, $p = 0.10$; left FFA ROI: $r(19) = -0.13$, $p = 0.57$. Taken together, the above results argue against motion being the explanatory factor for the differences we observed in the functional connectivity between the two conditions.

Matching Behavioral Performance and Pattern of Eye Fixations Between Configural and Featural Face Difference Detections

To ensure that the behavioral performance for featural and configural face difference detections was comparable, we conducted paired samples t-tests for both RT and accuracy (ACC) between these two task conditions. This analysis yielded no significant results (RT: $t(20) = 1.6$, $p = 0.10$; 1462 ms for configural difference detections; 1426 msec for featural difference detections; ACC: $t(20) = 1.06$, $p = 0.30$; 93% accuracy for configural difference detections; 92% accuracy for featural difference detections).

In the analyses of eye movements, number of fixations, fixation durations and duration to first fixation were the dependent measures with area of interest (AOI; see Methods) and type of face difference (featural or configural) as factors. All analyses were performed using linear mixed-effects models. The analysis on the number of fixations yielded a significant main effect of AOI ($F(15, 13\,775) = 1246$, $p < 0.01$) but not of type of face difference ($F(1, 13\,775) = 2$, $p = 0.15$), and there was no significant interaction between the factors ($F(15, 13\,775) = 0.5$, $p = 0.90$). The main effect of AOI showed that participants, irrespective of the type of face difference, mainly fixated the center and center-right AOIs of each face image, which corresponded to the position of the nose and right eye.

The analysis on the fixation duration data yielded similar results, with a significant main effect of AOI ($F(15, 13\,775) = 352$, $p < 0.01$) but not of type of face difference ($F(1, 13\,775) = 2$, $p = 0.15$), and there was no significant interaction between the factors ($F(15, 13\,775) = 0.56$, $p = 0.91$). The main effect of AOI indicated that fixations with the longest durations also occurred at the AOIs corresponding to the area around the nose and the right eye of a face.

The analysis on the duration to the first fixation yielded a significant main effect of AOI ($F(15, 13\,775) = 14$, $p < 0.01$) but not of type of face difference ($F(1, 13\,775) = 0.002$, $p = 0.97$), and there was no significant interaction between the factors ($F(15, 13\,775) = 0.75$, $p = 0.73$). Two AOIs comprised 90% of the first fixations and these again corresponded to the AOIs described above, namely, the center and center-right AOIs of each face image, which corresponded to the position of the nose and right eye. The average duration to the first fixation was 548 msec for configural difference detections and 554 ms for featural difference detections.

Lastly, we examined differences in the average saccade length between configural and featural difference detections. For this analysis, we used the same linear mixed-effects model described above, with type of face difference as the factor and average saccade length as the dependent measure. This analysis did not yield a significant main effect of type of face difference ($F(1, 986) = 0.62$, $p = 0.43$; average saccade length of 14.1° of visual angle for configural and 12.6° of visual angle for featural difference detections).

The eye-tracking data thus indicated that participants fixated the same within-face locations for the same amounts of time, regardless of whether the faces differed in configuration or features.

TMS Experiment

Localizer Tasks

Dorsal stream localizer task. We used the same dorsal stream localizer tasks used in the fMRI study to individually identify bilateral peaks of activity in response to same-different distance detections in relation to same-different brightness detections. These peaks of activity acted as the main TMS target sites in the left and right PPC. The vertex (also identified separately for each participant, see Methods) acted as the control site.

Main Task

To compare the effect of TMS applied over the left and right PPC and vertex on participants' behavioral performance in detecting configural and featural face differences, we used the same main-task procedure used in the fMRI study, but modified to comply with TMS safety requirements (see Methods). The main factors for the TMS study were as follows: TMS site (vertex, left or right PPC), TMS condition (administered or not), type of face difference (configural or featural) and session order (vertex first or PPC first).

In the analysis on RT, the main effects of TMS site [$F(2, 10\,737) = 8.9$, $p < 0.01$], TMS condition [$F(1, 11\,377) = 16.9$, $p < 0.01$] and type of face difference [$F(1, 11\,377) = 66$, $p < 0.01$] were significant. Session order was not a significant main effect [$F(1,19) = 0.77$, $p = 0.39$]. In addition, we found three significant two-way interactions: (1) TMS site by TMS condition, [$F(2, 11\,377) = 12$, $p < 0.01$]; (2) type of face difference by TMS condition, [$F(1, 11\,377) = 21$, $p < 0.01$]; and (3) type of face difference by TMS site [$F(2, 11\,377) = 15$, $p < 0.01$]. No significant interactions were observed between session order and the other factors: TMS site by session order [$F(2, 11\,377) = 1.02$, $p = 0.31$]; type of face difference by session order [$F(1, 11\,377) = 2.6$, $p = 0.12$]; TMS condition by session order [$F(1, 11\,377) = 1.3$, $p = 0.25$]. A significant three-way interaction was also observed, [$F(2, 11\,377) = 11$, $p < 0.01$], between TMS site, TMS condition, and type of face difference (Fig. 4A). The three- way interactions between the session order and the remaining factors were not significant: TMS

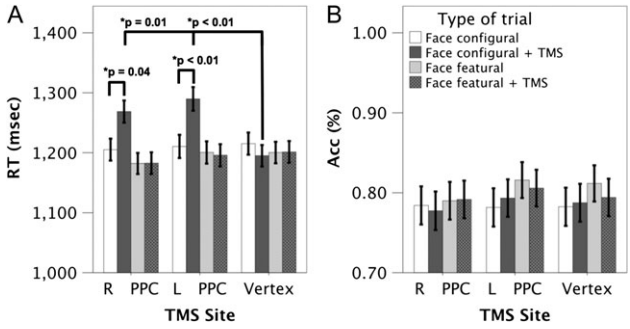

Figure 4. The figure depicts the behavioral data analysis of the TMS experiment, arranged by the type of trial. (A) Reaction Time (RT, in msec) and (B) Accuracy (ACC, % correct) across all the four different trial types of the TMS experiment. The three-way interaction between TMS site, type of face difference (configural/featural) and TMS (applied or not) in the analysis of RT is shown in (A). The abbreviations depicted on the x-axis are as follows: R PPC: right posterior parietal cortex; L PPC: left posterior parietal cortex. The error bars denote +/− 1 SE.

site by type of face difference by session order [$F(2, 11\ 377) = 0.34$, $p < 0.70$]; TMS site by TMS condition by session order [$F(2, 11\ 377) = 1.19$, $p < 0.30$]; type of face difference by TMS condition by session order [$F(1, 11\ 377) = 1.02$, $p < 0.31$]. The four-way interaction between session order and the remaining factors was also not significant $F(2, 11\ 377) = 0.75$, $p < 0.40$.

The analysis on accuracy yielded no significant main effects or interactions (Fig. 4B): [type of face difference $F(1, 14\ 358) = 2.3$, $p = 0.13$; TMS site: $F(2, 14\ 358) = 1.6$, $p = 0.2$; TMS condition: $F(1, 14\ 358) = 0.22$, $p = 0.64$; session order $F(1, 19) = 2.9$, $p = 0.11$; TMS condition by type of face difference: $F(1, 14\ 358) = 0.77$, $p = 0.38$; TMS site by type of face difference: $F(2, 14\ 358) = 0.21$, $p = 0.81$; TMS site by TMS condition: $F(2, 14\ 358) = 0.04$, $p = 0.96$; TMS site by TMS by type of face difference: $F(2, 14\ 358) = 1.14$, $p = 0.32$; Type of face difference by session order: $F(1, 14\ 358) = 3.0$, $p = 0.08$; TMS condition by session order: $F(1, 14\ 358) = 0.6$, $p = 0.44$; TMS site by session order: $F(2, 14\ 358) = 2.24$, $p = 0.11$; type of face difference by TMS condition by session order: $F(1, 14\ 358) = 0.01$, $p = 0.92$; type of face difference by TMS site by session order: $F(2, 14\ 358) = 1.8$, $p = 0.16$; TMS condition by TMS site by session order: $F(2, 14\ 358) = 1.15$, $p = 0.32$; type of face difference by TMS condition by TMS site by session order: $F(2, 14\ 358) = 0.91$, $p = 0.40$].

To understand the significant interactions observed in the RT data, we conducted two different sets of pair-wise comparisons between the factors. These pairwise comparisons are comparable to running several, paired *t*-tests but are, instead, run within the context of an omnibus ANOVA, by defining post-hoc contrasts. These post-hoc contrasts were adjusted for multiple comparisons using Sidak. In the first set of pairwise comparisons, we contrasted featural difference trials with and without TMS, and configural difference trials with and without TMS, separately for each TMS site (Fig. 4A). In this first analysis, trials with no TMS acted as the baseline, effectively testing the impact of TMS and how it varied across TMS sites.

For the left PPC, there was a significant difference between configural trials with and without TMS ($p < 0.01$), such that participants were slower to detect configural differences with TMS relative to those without TMS. In contrast, there was no significant difference between featural difference trials with and without TMS ($p = 1.0$). In addition, there was no significant difference between configural and featural difference trials without TMS ($p = 0.93$).

For the right PPC, the results were the same as those found for the left PPC: configural difference trials with TMS differed in RT from trials without TMS ($p = 0.04$), such that participants were slower on trials with TMS relative to trials without TMS. No difference was observed between featural difference detection trials with versus without TMS ($p = 1.0$) and there was no difference in RT between configural and featural trials without TMS ($p = 0.55$).

The analysis for the vertex site yielded no significant results (configural difference trials with vs. without TMS, $p = 0.98$; featural difference trials with vs. without TMS, $p = 0.96$; configural vs. featural difference trials without TMS, $p = 0.98$).

The above results thus indicate that participants were slower to detect configural differences on TMS trials compared to no TMS trials, but only when TMS was administered over the left or right PPC sites. TMS had no effect when delivered to the vertex and had no impact on featural difference detections irrespective of the TMS site. Accuracy was not affected by TMS, irrespective of the type of face difference or the TMS site. Lastly, configural and featural face difference detections without TMS did not differ in RT or accuracy across TMS sites, indicating that the two tasks were matched for difficulty.

In the second set of pair-wise comparisons, we contrasted trials from the left/right PPC and vertex TMS sites, separately for featural difference trials with and without TMS, and configural difference trials with and without TMS. In this second analysis, trials from the control vertex site, rather than trials without TMS, served as the baseline, which allowed for the direct comparison of the effect of TMS between the left and right PPC and the vertex sites.

The analysis on configural difference trials with TMS showed significant differences between the left PPC and vertex ($p < 0.01$), as well as between the right PPC and vertex ($p = 0.01$; Fig. 4A). No significant difference was observed between the left and right PPC sites ($p = 0.20$). In contrast to the analysis on configural difference detections, featural difference trials with TMS were not significantly different between TMS sites (left PPC vs. vertex, $p = 0.98$; right PPC vs. vertex, $p = 0.55$; left vs. right PPC, $p = 0.56$).

As anticipated, trials without TMS did not differ between TMS sites, irrespective of the type of face difference (configural face differences: left PPC vs. vertex, $p = 0.95$; right PPC vs. vertex, $p = 0.92$; left vs. right PPC, $p = 1.00$; featural face differences: left PPC vs. vertex, $p = 0.42$; right PPC vs. vertex, $p = 0.32$; left vs. right PPC, $p = 0.56$).

The results of the above analysis confirmed that, for the TMS sites we identified, TMS was only effective on configural difference detections and only for regions of the dorsal stream.

Discomfort Ratings

At the end of each TMS session, participants rated the discomfort they felt during TMS, separately for each TMS site, on a ten-point scale (1 slightly uncomfortable, 10 very uncomfortable). The results indicated that discomfort ratings were uniformly low and comparable across TMS sites ($F(2,59) = 0.18$, $p = 0.83$; average discomfort rating: left PPC 2.50, right PPC 2.60, vertex 2.40). Hence, TMS effects could not be attributed on differences in discomfort between TMS sites.

Discussion

Processing the configuration and shape of facial features are considered to be integral aspects of face perception mediated by

neural substrates within the ventral visual pathway (Yovel and Kanwisher 2004; Maurer et al. 2007; Pitcher et al. 2007; Liu et al. 2010; Zhang et al. 2012, 2015). If configural processing depends on fine-grained spatial information, do mechanisms within the dorsal visual pathway also contribute to this process? We explored this question in fMRI and TMS experiments, using configural and featural face difference detection tasks similar to those used previously (Yovel and Kanwisher 2004; Duchaine et al. 2006; Yovel and Duchaine 2006; Maurer et al. 2007; Pitcher et al. 2007; Barton 2008; Liu et al. 2010; Renzi et al. 2013).

We present two novel findings. First, spatial-processing regions within the dorsal visual pathway are involved in the configural processing of faces: (i) these regions were activated more strongly in response to configural face difference detections compared to featural face difference detections. (ii) The magnitude of the fMRI activity related to configural difference detections predicted the participants' RT on the configural face task. (iii) Critically, the right FFA (defined at the individual participant level) showed greater functional connectivity with the spatial-processing regions of the dorsal stream during configural face difference detections and greater functional connectivity with the left FFA during featural face difference detections.

Second, the spatial-processing regions within the dorsal visual pathway contribute to the configural processing of faces: TMS centered on these dorsal stream regions, in either the left or right hemisphere, significantly impaired the detection of configural face difference detections, but had no effect on featural face difference detections. Importantly, no effects were observed for the control TMS site, the vertex. Taken together, the fMRI and TMS findings provide compelling evidence for the contribution of posterior parietal regions to configural face processing.

Given that detecting differences in the configuration and in the shape of the facial features were matched for difficulty, and that the visual display and pattern of eye fixations did not differ for the two tasks, one cannot attribute the results to differential task demands or eye movements.

Collectively, our findings show that the dorsal visual pathway mediates a fundamental aspect of face perception, namely, the configural processing of facial features. More broadly, our findings provide novel, causal evidence that regions outside the ventral visual pathway can contribute to certain aspects of face perception. The findings, thus, have important implications for patients with lesions of PPC: one would predict face-processing impairments. Although the face-processing capacity of patients with PPC lesions is not routinely examined, there is intriguing evidence in the literature to support the above prediction.

One piece of evidence comes from patient RM, who suffered bilateral posterior parietal damage resulting from two separate strokes and subsequently exhibited severe visuospatial impairments (Robertson et al. 1997; Friedman-Hill et al. 2003). Patient RM, however, was also impaired in certain aspects of face perception: when presented with schematic drawings of faces, comprised of circles for the eyes and outline of the face, a line for the nose and a curve for the mouth, RM did not always identify the drawings as faces. In some test sessions, he described the drawings in the following way: "There is one big circle and one and a half little circles" or "I see one "O" (the letter "O") and a "T" (the letter "T") outside the big circle" (Robertson et al. 1997). RM's descriptions suggest that he was unable to perceive the face drawings as unified wholes (or gestalts) but instead relied on intact low-level processing of individual visual features.

Additional evidence comes from studies of face perception in patients with Williams's syndrome. Williams's syndrome is a rare, genetically-based neurodevelopmental disorder, associated with the abnormal development of PPC and a profound impairment in spatial cognition (Bellugi et al. 2000; Meyer-Lindenberg et al. 2006). Although face perception in William's syndrome patients is frequently reported as normal (Bellugi et al. 2000; Karmiloff-Smith et al. 2004; Meyer-Lindenberg et al. 2006), a close examination of the literature reveals specific face-related deficits in configural processing of upright faces and reduced sensitivity to the face inversion effect relative to age-matched controls (Karmiloff-Smith et al. 2004; Nakamura et al. 2013). There is actually a long-standing debate (Karmiloff-Smith et al. 2004) in the William's syndrome literature of whether or not face perception impairments are associated with this disorder and, more specifically, with an abnormally developing PPC.

Lastly, regions within the PPC are also implicated in studies of prosopagnosia. For example, Degutis et al. (Degutis et al. 2007) studied a developmental prosopagnosic patient who recovered from his disorder after training on a face-matching task, in which faces differed in the spacing of their internal features. This patient is unique in that prosopagnosic patients very rarely recover, irrespective of training. However, this patient showed improvement in face matching, post-training, which was accompanied by an increase in the functional connectivity between face-selective regions, as well as between the right FFA, right OFA and the right superior parietal lobule within PPC. The latter finding thus suggests that robust functional connectivity between face-processing regions of the ventral stream and regions within the PPC might together be necessary for veridical face perception.

Collectively, the above evidence supports our findings by indicating that, along with the contributions of the ventral visual pathway, the dorsal visual pathway may also contribute to certain aspects of face perception. A number of potential concerns, however, still remain. For instance, in the analysis of brain activity–RT correlations, brain activity within the ventral stream ROIs did not predict the participants' behavioral performance. By running subsequent analyses, we established that this lack of significant brain activity–RT correlation was not due to poor signal or low variability in the magnitude of brain activity within these regions. Consequently, it could be the case that the magnitude of activity within face processing regions of the ventral stream, such as the right FFA, is dependent not on task performance but rather on the category of the stimuli. For instance, activity within the right FFA is maximal in response to face stimuli and much less in response to non-face categories of objects (Kanwisher et al. 1997). Crucially, this category selectivity of face processing regions persists even when behavior is severely impaired: patients with developmental prosopagnosia are severely impaired in face perception but their right FFA and other occipitotemporal face processing regions show a normal magnitude of fMRI activation in response to faces, as compared to healthy controls (Avidan et al. 2005). Consequently, the behavioral correlates of face perception may be related to factors other than the magnitude of activity in ventral steam face processing regions, such as the pattern of activity associated with different face identities (e.g. Zhang et al. 2015; Nestor et al. 2016).

Unlike the ventral stream face processing regions, which are category-specific, the dorsal stream location processing regions are more process-specific, mediating spatial location processing irrespective of the stimulus category (Sereno and Lehky 2010). As such, the magnitude of activity within these dorsal stream regions may well dictate participants' performance in

spatial judgments, consistent with the significant brain activity–RT correlation observed in these regions.

Another potential concern is that configural face processing may have been erroneously considered a face-specific process, both here and in prior studies. That is, configural face processing may simply be a visuospatial process that is not associated with face perception per se. We think this possibility is very unlikely for the following reasons. First, it has been demonstrated here and in previous studies (Yovel and Kanwisher 2004; Maurer et al. 2007) that configural face difference detections engage face-selective areas (specifically, the right FFA) as strongly as featural face difference detections. In addition, using the same-different face detection control tasks, we demonstrated that individually localized FFA was activated in response to configural face difference detections as strongly as when the same participants performed same-different judgments between completely different faces. If the configural condition in the task were not a face task, one would have expected reduced activation to configural relative to featural difference detections and relative to same-different judgments between different faces, but this was not found. Additionally, we found identical eye-fixation patterns between the configural and featural face tasks, indicating that participants did not use differential strategies between these two tasks.

Second, it has been demonstrated behaviorally (Leder and Bruce 2000; Yovel and Kanwisher 2004; Rossion 2008) and in fMRI (Yovel and Kanwisher 2004) that configural face tasks, like the one used here, are as susceptible to the face inversion effect as featural tasks, relative to tasks involving non-face categories of objects (e.g. houses). The face inversion effect is the most fundamental effect in support of the domain-specific nature of faces. Consequently, it is highly unlikely that the face-specific inversion effect would be observed if configural face difference detections were processed as a non-face category.

Third, prosopagnosic patients are especially poor at configural face difference detections compared to controls (Le Grand et al. 2006; Yovel and Duchaine 2006; Barton 2008). If faces in configural processing could be treated as a non-face category, then prosopagnosic patients should not have been as impaired since they can discriminate differences in configuration between non-face categories of objects (Yovel and Duchaine 2006).

Taken together, the studies we summarize here demonstrate that configural face processing is not a simple visuospatial process but rather a face-specific process that depends on the face-processing substrates of the ventral visual pathway. Our experiments extend these findings to show that configural face processing requires fine-grained spatial information that is processed, at least in part, by spatial-processing mechanisms within the dorsal visual pathway. Exactly how dorsal spatial information is integrated with other face-related information remains to be determined. Based on the results from our functional connectivity analysis, one possibility is that the integration of featural and configural information results from information exchange between the right FFA and spatial processing regions in posterior parietal cortex. A ventral-dorsal exchange of information is compatible with previous work indicating that the functional independence of the two visual pathways may not be absolute (Ross and Dickinson, 2007; Kravitz et al. 2013; Freud et al. 2015).

Funding

National Institute of Mental Health Intramural Research Program (NIH Clinical Study Protocol 93-M-0170, NCT00001360).

Notes

We wish to thank the NIH Fellows Editorial Board for assistance with the preparation of the manuscript. *Conflict of Interest:* None declared.

References

Avidan G, Hasson U, Malach R, Behrmann M. 2005. Detailed exploration of face-related processing in congenital prosopagnosia: 2. Functional neuroimaging findings. J. Cognitive Neurosci. 17:1150–67.

Barton JJ. 2008. Structure and function in acquired prosopagnosia: lessons from a series of 10 patients with brain damage. J Neuropsychol. 2:197–225.

Behzadi Y, Restom K, Liau J, Liu TT. 2007. A component based noise correction method (CompCor) for BOLD and perfusion based fMRI. Neuroimage. 37:90–101.

Bellugi U, Lichtenberger L, Jones W, Lai Z, St George M. 2000. I. The neurocognitive profile of Williams Syndrome: a complex pattern of strengths and weaknesses. J Cogn Neurosci. 12:7–29.

Busigny T, Graf M, Mayer E, Rossion B. 2010. Acquired prosopagnosia as a face-specific disorder: ruling out the general visual similarity account. Neuropsychologia. 48:2051–2067.

Chen G, Saad ZS, Britton JC, Pine DS, Cox RW. 2013. Linear mixed-effects modeling approach to FMRI group analysis. Neuroimage. 73:176–190.

Cox RW. 1996. AFNI: software for analysis and visualization of functional magnetic resonance neuroimages. Comput Biomed Res. 29:162–173.

DeGutis JM, Bentin S, Robertson LC, D'Esposito M. 2007. Functional plasticity in ventral temporal cortex following cognitive rehabilitation of a congenital prosopagnosic. J Cogn Neurosci. 19:1790–1802.

Della Sala S, Young AW. 2003. Quaglino's 1867 case of prosopagnosia. Cortex. 39:533–540.

Domagalik A, Beldzik E, Oginska H, Marek T, Fafrowicz M. 2014. Inconvenient correlation–RT–BOLD relationship for homogeneous and fast reactions. Neuroscience. 278:211–221.

Duchaine BC, Yovel G, Butterworth EJ, Nakayama K. 2006. Prosopagnosia as an impairment to face-specific mechanisms: Elimination of the alternative hypotheses in a developmental case. Cogn Neuropsychol. 23:714–747.

Fox CJ, Iaria G, Barton JJ. 2009. Defining the face processing network: optimization of the functional localizer in fMRI. Hum Brain Mapp. 30:1637–1651.

Freud E, Ganel T, Shelef I, Hammer MD, Avidan G, Behrmann M. 2015. Three-Dimensional Representations of Objects in Dorsal Cortex are Dissociable from Those in Ventral Cortex. Cerebral Cortex. 1:13.

Friedman-Hill SR, Robertson LC, Desimone R, Ungerleider LG. 2003. Posterior parietal cortex and the filtering of distractors. Proc Natl Acad Sci USA. 100:4263–4268.

Gauthier I, Hayward WG, Tarr MJ, Anderson AW, Skudlarski P, Gore JC. 2002. BOLD activity during mental rotation and viewpoint-dependent object recognition. Neuron. 34:161–171.

Gotts SJ, Saad ZS, Jo HJ, Wallace GL, Cox RW, Martin A. 2013. The perils of global signal regression for group comparisons: a case study of Autism Spectrum Disorders. Front Hum Neurosci. 7:52–71.

Gotts SJ, Simmons WK, Milbury LA, Wallace GL, Cox RW, Martin A. 2012. Fractionation of social brain circuits in autism spectrum disorders. Brain. 135:2711–2725.

Harris A, Aguirre GK. 2010. Neural tuning for face wholes and parts in human fusiform gyrus revealed by FMRI adaptation. J Neurophysiol. 104:336–345.

Haxby JV, Grady CL, Horwitz B, Ungerleider LG, Mishkin M, Carson RE, Herscovitch P, Schapiro MB, Rapoport SI. 1991. Dissociation of object and spatial visual processing pathways in human extrastriate cortex. Proc Natl Acad Sci USA. 88:1621–1625.

Haxby JV, Hoffman EA, Gobbini MI. 2000. The distributed human neural system for face perception. Trends Cogn Sci. 4:223–233.

Jo HJ, Saad ZS, Simmons WK, Milbury LA, Cox RW. 2010. Mapping sources of correlation in resting state FMRI, with artifact detection and removal. Neuroimage. 52:571–582.

Kanwisher N, McDermott J, Chun MM. 1997. The fusiform face area: a module in human extrastriate cortex specialized for face perception. J Neurosci. 17:4302–4311.

Karmiloff-Smith A, Thomas M, Annaz D, Humphreys K, Ewing S, Brace N, Duuren M, Pike G, Grice S, Campbell R. 2004. Exploring the Williams syndrome face-processing debate: the importance of building developmental trajectories. J Child Psychol Psychiatry. 45:1258–1274.

Kimchi R, Behrmann M, Avidan G, Amishav R. 2012. Perceptual separability of featural and configural information in congenital prosopagnosia. Cognitive Neuropsych. 29:447–463.

Kravitz DJ, Saleem KS, Baker CI, Ungerleider LG, Mishkin M. 2013. The ventral visual pathway: an expanded neural framework for the processing of object quality. Trends Cogn Sci. 17:26–49.

Le Grand R, Cooper PA, Mondloch CJ, Lewis TL, Sagiv N, de Gelder B, Maurer D. 2006. What aspects of face processing are impaired in developmental prosopagnosia? Brain Cogn. 61:139–158.

Leder H, Bruce V. 2000. When inverted faces are recognized: the role of configural information in face recognition. Q J Exp Psychol. 53:513–536.

Liu J, Harris A, Kanwisher N. 2010. Perception of face parts and face configurations: an fMRI study. J Cogn Neurosci. 22:203–211.

Maurer D, Le Grand R, Mondloch CJ. 2002. The many faces of configural processing. Trends Cogn Sci. 6:255–260.

Maurer D, O'craven KM, Le Grand R, Mondloch CJ, Springer MV, Lewis TL, Grady CL. 2007. Neural correlates of processing facial identity based on features versus their spacing. Neuropsychologia. 45:1438–1451.

Meyer-Lindenberg A, Mervis CB, Berman KF. 2006. Neural mechanisms in Williams syndrome: a unique window to genetic influences on cognition and behavior. Nat Rev Neurosci. 7:380–393.

Mishkin M, Ungerleider LG, Macko KA. 1983. Object vision and spatial vision: two cortical pathways. Trends Neurosci. 6:414–417.

Nakamura M, Watanabe S, Inagaki M, Hirai M, Miki K, Honda Y, Kakigi R. 2013. Electrophysiological study of face inversion effects in Williams syndrome. Brain and Dev. 35:323–330.

Nestor A, Plaut DC, Behrmann M. 2016. Feature-based face representations and image reconstruction from behavioral and neural data. Proc Natl Acad Sci. 113:416–421.

Olesen PJ, Westerberg H, Klingberg T. 2004. Increased prefrontal and parietal activity after training of working memory. Nat Neurosci. 7:75–79.

Pitcher D, Walsh V, Yovel G, Duchaine B. 2007. TMS evidence for the involvement of the right occipital face area in early face processing. Curr Biol. 17:1568–1573.

Rao NK, Motes MA, Rypma B. 2013. Investigating the neural bases for intra-subject cognitive efficiency changes using functional magnetic resonance imaging. Front Hum Neurosci. 8:840–840.

Renzi C, Schiavi S, Carbon CC, Vecchi T, Silvanto J, Cattaneo Z. 2013. Processing of featural and configural aspects of faces is lateralized in dorsolateral prefrontal cortex: a TMS study. Neuroimage. 74:45–51.

Robertson L, Treisman A, Friedman-Hill S, Grabowecky M. 1997. The interaction of spatial and object pathways: evidence from Balint's syndrome. J Cogn Neurosci. 9:295–317.

Ross J, Dickinson JE. 2007. Effects of adaptation to Glass pattern structure and to path of optic flow. Vision Res. 47:2150–2155.

Rossi S, Hallett M, Rossini PM, Pascual-Leone A, Safety of TMS Consensus Group. 2009. Safety, ethical considerations, and application guidelines for the use of transcranial magnetic stimulation in clinical practice and research. Clin Neurophysiol. 120:2008–2039.

Rossion B. 2008. Picture-plane inversion leads to qualitative changes of face perception. Acta Psychol. 128:274–289.

Rossion B, Caldara R, Seghier M, Schuller AM, Lazeyras F, Mayer E. 2003. A network of occipito-temporal face-sensitive areas besides the right middle fusiform gyrus is necessary for normal face processing. Brain. 126:2381–2395.

Rossion B, Dricot L, Devolder A, Bodart J, Crommelinck M, Gelder BD, Zoontjes R. 2000. Hemispheric asymmetries for whole-based and part-based face processing in the human fusiform gyrus. J Cogn Neurosci. 12:793–802.

Saad ZS, Reynolds RC, Jo HJ, Gotts SJ, Chen G, Martin A, Cox RW. 2013. Correcting brain-wide correlation differences in resting-state FMRI. Brain Connect. 3:339–352.

Sereno AB, Lehky SR. 2010. Population coding of visual space: comparison of spatial representations in dorsal and ventral pathways. Front Comput Neurosci. 4:159.

Sergent J, Ohya S, Macdonald B. 1992. Functional neuroanatomy of face and object processing. A positron emission tomography study. Brain. 115:15–36.

Silson EH, McKeefry DJ, Rodgers J, Gouws AD, Hymers M, Morland AB. 2013. Specialized and independent processing of orientation and shape in visual field maps LO1 and LO2. Nat. Neurosci. 16:267–269.

Stoddard J, Gotts SJ, Brotman MA, Lever S, Hsu D, Zarate C, Ernst M, Pine DS, Leibenluft E. 2016. Aberrant intrinsic functional connectivity within and between corticostriatal and temporal-parietal networks in adults and youth with bipolar disorder. Psychol Med. 1:1–14.

Talairach J, Tournoux P. 1988. Co-planar stereotaxic atlas of the human brain. 3-Dimensional proportional system: an approach to cerebral imaging. Stuttgart (Germany) & New York (NY): Thieme Verlag.

Taubert J, Apthorp D, Aagten-Murphy D, Alais D. 2011. The role of holistic processing in face perception: evidence from the face inversion effect. Vision Res. 51:1273–1278.

Ungerleider LG, Mishkin M. 1982. Two cortical visual systems. In: Ingle DJ, Goodale MA, Mansfield RJW, editors. Analysis of visual behavior. Boston (MA): MIT Press. p. 549–586.

Voßkühler A. 2009. OGAMA description (for Version 2.5). Berlin: Freie Universität Berlin, Germany. Fachbereich Physik.

Wassermann EM. 1998. Risk and safety of repetitive transcranial magnetic stimulation: report and suggested guidelines from the International Workshop on the Safety of Repetitive Transcranial Magnetic Stimulation, June 5–7, 1996. Electroencephalogr Clin Neurophysiol. 108:1–16.

Yarkoni T, Barch DM, Gray JR, Conturo TE, Braver TS. 2009. BOLD correlates of trial-by-trial reaction time variability in gray and white matter: a multi-study fMRI analysis. PLoS One. 4:e4257.

Yovel G, Duchaine B. 2006. Specialized face perception mechanisms extract both part and spacing information: evidence from developmental prosopagnosia. J Cogn Neurosci. 18: 580–593.

Yovel G, Kanwisher N. 2004. Face perception: domain specific, not process specific. Neuron. 44:889–898.

Zachariou V, Nikas V, Safiullah ZN, Behrmann M, Klatzky R, Ungerleider LG. 2015. Common dorsal stream substrates for the mapping of surface texture to object parts and visual spatial processing. J Cogn Neurosci. 27: 2442–2461.

Zhang J, Li X, Song Y, Liu J. 2012. The fusiform face area is engaged in holistic, not parts-based, representation of faces. PLoS One. 7:e40390.

Zhang J, Liu J, Xu Y. 2015. Neural decoding reveals impaired face configural processing in the right fusiform face area of individuals with developmental prosopagnosia. J Neurosci. 35:1539–1548.